Optimization of the Syngas Combustion Chemistry Model

Rui Xu[*]

Department of Mechanical Engineering, Stanford University, Stanford, CA 94305

[*] Email: ruixu@stanford.edu

Project category: physical science

Team member: Rui Xu (SUNet ID: ruixu; SUID: 05793976)

Abstract

Practically, an accurate combustion chemistry model is of great importance in engine simulations when it is combined with the computational fluid dynamics computations. Syngas is used as one of the fuel options in internal combustion engines. In the current work, we optimize a combustion chemistry model of syngas using machine learning algorithms. Result shows that the optimized model can achieve better prediction accuracy than the unoptimized model.

1. Introduction

Synthetic gas (syngas) consists of hydrogen (H_2) and carbon monoxide (CO), sometimes with carbon dioxide (CO_2). It is used as one of the fuel options in internal combustion engines. From engine design perspective, it is very important to understand the process of syngas combustion process inside the engine, through combining the computational fluid dynamics (CFD) simulation with the combustion chemistry model. A typical syngas combustion chemistry model contains about 10-15 species and 30 reactions. In each reaction j (j = 1, 2, …, n), a parameter called reaction rate coefficient k_j is assigned, describing how fast this certain reaction evolves in the system. The rate parameter k can be either obtained from fundamental chemical kinetic experiments, or from quantum chemistry calculations. To validate the rate parameters, the chemistry model will be implemented with a Fortran solver, ChemKin [1], to simulate the time evolution or spatial evolution of the combustion system, and provide a wide range of predictions, such as combustion product yield, ignition delay time, laminar flame speed, etc. The model predictions can be directly compared with experimental measurements to validate the model accuracy. However, such combustion chemistry model with initial rate parameters determined independently may sometimes provide inaccurate predictions, because those parameters fail to consider the chemical kinetic couplings between each other. Therefore, people rely on slight modifications to certain rate parameters, in order to better reproduce the experimental data. Considering a reaction model with 30 parameters and the coupling between each other, the aforementioned "rate tuning" approach becomes a daunting task.

In the present work, we apply the machine learning theory and algorithms to optimize a combustion chemistry model of syngas. The syngas model is first built with rate coefficients determined based on old literatures and some earlier empirical estimations, which is also called the unoptimized trial model. Then, the model responses from ChemKin solver are mapped into second-order response surfaces. Finally, the model is optimized using global combustion experimental data. The inputs are the rate coefficient k in the model, and the output is the chemistry model response. We used two machine learning approaches to optimize the model: locally weighted least square and reinforcement learning. Result shows that the optimized model can achieve better prediction accuracy than the original model.

2. Experimental Dataset

In the current work, some typical global combustion data from H_2, CO, and syngas combustion experiments are selected from earlier literatures [2-12]. The combustion properties considered in this work are: species concentration time history profile, ignition delay time, and laminar flame speed. Figure 1 shows selected experimental sets of species profile, ignition delay time, and laminar flame speed, respectively. The data used in this work are extracted from the full datasets, which are highlighted as open squares in Figure 1. Specifically, the species profile and flame speed data are directly selected from the original dataset. The ignition delay time data are extracted

from the linear fitted log of ignition time vs. 1/T correlations. In total, we extracted 200 experimental data points from the literature.

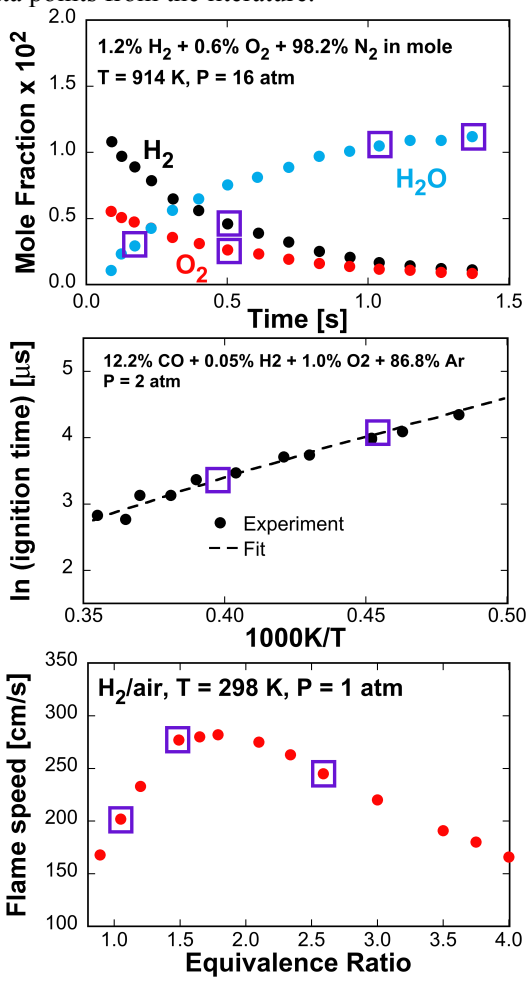

Figure 1. Selected experimental dataset. Top panel: species concentration profiles [12]; middle panel: ignition delay time [9]; bottom panel: laminar flame speed [2].

3. Methodology

The current work consists of three parts: feature selection, solution mapping, and model optimization. A schematic of the work flow is illustrated in Figure 2.

3.1. Feature selection

As stated in the introduction section, the features in this work are the rate parameters, k_j of each reaction j ($j = 1, 2, \ldots, n$). To start, we build an initial trial model for syngas, and the rate parameters are obtained from some earlier literatures and empirical estimates [13-15]. The initial model is shown in Table 1. Note that for each reaction, the reaction rate coefficient is related to three physical parameters, A, n, and E_a, through Equation (1) shown below:

$$k = AT^n exp\left(\frac{-E_a}{RT}\right) \quad (1)$$

The uncertainty factor f values in Table 1 are obtained from an earlier work [16]. The initial model contains 13 chemical species and 30 reactions. In fact, we can further reduce the number of features through a set of sensitivity analysis using the ChemKin solver. Typically, in the combustion system, not all the reactions contribute equally to the combustion products or global oxidation properties. In fact, only a few reactions are dominant. Therefore, we use the ChemKin package to perform sensitivity analysis with respect to the experimental condition of each data point. Among the 30 reactions in the model, only 10 reactions are found to be effective to all the 200 experimental conditions and data points. The effective reactions are highlighted in red in Table 1. In such way, we reduced the number of features from 30 to 10.

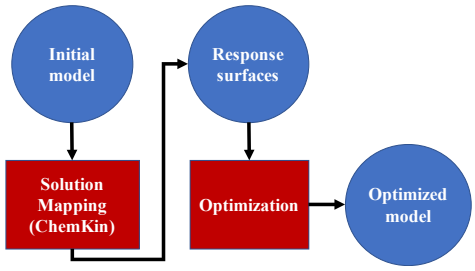

Figure 2. Schematic of the current work.

Table 1. The unoptimized chemical model of syngas.

No.	Reactions	Reaction rate coefficients			Uncertainty factor, f
		A (mol/cm^3.s)	n	E_a (cal/mol)	
1	H+O2 = O+OH	2.65E+16	-0.671	17041.0	1.15
2	O+H2 = H+OH	3.87E+04	2.700	6260.0	1.3
3	OH+H2 = H+H2O	2.16E+08	1.510	3430.0	1.3
4	OH+OH = O+H2O	3.57E+04	2.400	-2110.0	1.3
5	H+H+M = H2+M	1.00E+18	-1.000	0.0	2
6	H+H+H2 = H2+H2	2.20E+22	-2.000	0.0	2
7	H+H+H2O = H2+H2O	4.71E+18	-1.000	0.0	2
8	H+H+CO2 = H2+CO2	1.20E+17	-1.000	0.0	2
9	H+OH+M = H2O+M	4.65E+12	0.440	0.0	1.2
10	O+H+M = OH+M	7.40E+05	2.433	53502.0	1.25
11	O+O+M = O2+M	7.40E+13	-0.370	0.0	1.5
12	H+O2(+M) = HO2(+M)	3.97E+12	0.000	671.0	1.5
13	H2+O2 = HO2+H	7.08E+13	0.000	295.0	2
14	OH+OH(+M) = H2O2(+M)	2.00E+13	0.000	0.0	2
15	HO2+H = O+H2O	2.90E+13	0.000	-500.0	2
16	HO2+H = OH+OH	1.30E+11	0.000	-1630.0	1.5
17	HO2+O = OH+O2	1.21E+07	2.000	5200.0	2
18	HO2+HO2 = O2+H2O2	2.41E+13	0.000	3970.0	2
19	OH+HO2=H2O+O2	9.63E+06	2.000	3970.0	2
20	H2O2+H = HO2+H2	2.00E+12	0.000	427.0	2
21	H2O2+H = OH+H2O	1.80E+10	0.000	2384.0	2
22	H2O2+O = OH+HO2	7.05E+04	2.053	-355.7	2
23	H2O2+OH = HO2+H2O	2.53E+12	0.000	47700.0	3
24	CO+O(+M) = CO2(+M)	3.01E+13	0.000	23000.0	2
25	CO+OH = CO2+H	1.20E+14	0.000	0.0	2
26	CO+O2 = CO2+O	3.00E+13	0.000	0.0	2
27	CO+HO2 = CO2+OH	3.00E+13	0.000	0.0	2
28	HCO+H = CO+H2	3.02E+13	0.000	0.0	2
29	HCO+O = CO+OH	9.35E+16	-1.000	17000.0	2
30	HCO+O = CO2+H	1.20E+10	0.807	-727.0	2

3.2. Solution Mapping

The optimization process requires the comparison between experimental data and simulated results using the chemistry model. However, it is computationally inefficient to simulate through the ChemKin solver each and every time, especially when optimizing the model using reinforcement learning approach. Instead, we want to map our ChemKin solution into some simple mathematical formula, and in doing so, we could boost up the optimization process dramatically.

Consider a combustion system output y (e.g. ignition delay time and flame speed), which is related to the system input x (reaction rate parameters k), through a mathematical relation, $y = g(x)$. Numerically, y is obtained by solving several coupled partial differential equations, so the relation g, which is highly complex, might not be determined analytically. However, one can perform an estimation of y which resembles a Taylor expansion:

$$y = c + \sum_{j=1}^{n} b_j x_j + \sum_{j=1}^{n}\sum_{k\geq j}^{n} a_{jk} x_j x_k + H.O.T. \qquad (2)$$

where x_j is the j^{th} element of input x, a_{jk}, b_j, and c are coefficients of the 2nd, 1st and 0 order terms. Applying Eqn. (2) to the combustion system, the coefficient c represents some nominal value of system output y. The first order terms represent the first-order effect of reaction rate coefficients to the system. Higher order terms accounts for the coupled effects of rate parameters to the system. In this study, we only consider the first- and second-order effects, and neglect any higher order effects. Therefore, For the i^{th} experimental data point, the model response $\eta_{resp}^{(i)}$ can be written as follows:

$$\begin{aligned}\eta_{resp}^{(i)} &= c^{(i)} + \sum_{j=1}^{n} b_j^{(i)} x_j^{(i)} + \sum_{j=1}^{n}\sum_{k\geq j}^{n} a_{jk}^{(i)} x_j^{(i)} x_k^{(i)} \\ &= c^{(i)} + \left(b^{(i)}\right)^T x + x^T A^{(i)} x\end{aligned} \qquad (3)$$

The process of the model response surface derivation will be discussed in detail in the results section.

3.3. Model Optimization

3.3.1. Approach 1: Locally weighted least square

Suppose we've already obtained accurate response surfaces for all the data points (experimental conditions), the next step is to perform a locally weighted least square and solve for x_{opt}. In other words, we perform the following optimization:

$$\min_x J(x) = \sum_{i=1}^{m}\left[\frac{\left(\eta_{resp}^{(i)} - \eta_{expt}^{(i)}\right)}{\sigma_{expt}^{(i)}}\right]^2 \qquad (4)$$

where $\eta_{expt}^{(i)}$ is the i^{th} training data point, $\eta_{resp}^{(i)}$ is the response surface predicted value for the i^{th} data point, and $\sigma_{expt}^{(i)}$ is the measurement uncertainty associated to the i^{th} experiment, which is usually reported as error bars or tabulated values in literatures. To perform the optimization described in Eqn. (4), we simply run gradient descent method. Since $\eta_{resp}^{(i)}$ can be represented by Eqn. (2), then $J(x)$ turns into:

$$J(x) = \sum_{i=1}^{m}\left[\frac{\left(c^{(i)} + \left(b^{(i)}\right)^T x + x^T A^{(i)} x - \eta_{expt}^{(i)}\right)}{\sigma_{expt}^{(i)}}\right]^2 \qquad (5)$$

The gradient of $J(x)$ with respect to x_j can be calculated as:

$$\frac{\partial J}{\partial x_j} = \sum_{i=1}^{m} 2\frac{(\eta_{resp}^{(i)} - \eta_{expt}^{(i)})}{(\sigma_{expt}^{(i)})^2}(b_j^{(i)} + A^{(i)}x) \qquad (6)$$

Then, we can perform either the batch gradient descent or stochastic gradient descent method to update the parameter x_j. In this work, stochastic gradient descent approach is used here for fast convergence.

3.3.2. Approach 2: Reinforcement learning

As mentioned in the introduction section, when the initially assembled chemistry model does not reproduce the experimental data, people tend to fine tune a certain number of rate parameters in order to match the data. However, this might lead to a situation where the modified model does reproduce the data mentioned above, but fails to predict another set of data. Then people again adjust a different set of rate coefficients. Finally, this fine-tuning process becomes boring and daunting. Indeed, the model fine-tuning process resembles a Markov decision process (MDP). We start with an initial model, and this model might be able to reproduce a certain set of experimental data, while fail to capture another set of data. Then, we make adjustments to the reaction rate coefficients, expecting that through modifying a certain set of rata parameters, the uncaptured data can be reproduced by the modified model. As a result of this modification, the new state of MDP would transition to a new state that cannot be predicted by users.

Based on the intuition just discussed, we define our MDP as the followings:

- The state set S, is the set of all the combinations of model predictions of each experimental data. Specifically, for each data point, the chemistry model should either predicts it within its uncertainty band, or fails to reproduce the data point, including either overpredicting or underpredicting it. In other words, for each data point, the model prediction will have three outcomes, and for totally m data points, the size of the state set S should be $|S| = 3^m$.
- For the actions, let's look at one single reaction in the chemistry model. To modify the model, we can either increase the reaction rate parameter, or decrease it, by say 20 % of its uncertainty factor f (see Table 1). For n effective reactions, the size of the state set A should be $|A| = 2^n$.
- P_{sa} are the state transition probabilities, which is a $3^m \times 3^m \times 2^n$ matrix.
- $R(s)$ is the reward function. After each action, we check whether the model can predict all the data points within their uncertainty bands. If yes, we reach the success state in S, and a positive reward will be assigned. On the other hand, if there is at least one data point which is not predicted, we assign a negative reward to the value function.
- The value function $V^{\pi}(s)$ is updated using value iteration method to solve the Bellman equation:

$$V^{\pi}(s) = R(s) + \gamma \sum_{s' \in S} P_{s\pi(s)}(s')\, V^{\pi}(s') \qquad (7)$$

- Finally, the MDP stops when the learning procedure converges once for a certain number of consecutive trials, or our total number of successes exceeds a certain limit. Then we save the last rate parameters x as x_{opt}.

4. Results and Discussions

4.1. Model Response Surface Generation

Before we start generating the response surfaces, the rate parameter k is normalized into x through the following way:

$$x = \ln\left(\frac{k}{k_0}\right) / \ln(f) \qquad (8)$$

where k is the reaction rate in each reaction with nominal value k_0, and f is its uncertainty factor. For the unoptimized model, since $k = k_0$, then initially $x = 0$ for each reaction. The purpose of this normalization is for numerical convenience, since the original k can vary wildly in orders of magnitude.

The response surfaces are derived based on a Monte Carlo sampling process. For example, each data point corresponds to an experimental condition (e.g. initial temperature, pressure, and reactant concentrations). Take the i^{th} data point (experimental condition) as an example, we randomly generate q chemistry models. In each random model, the rate parameters are randomly chosen within their rate uncertainty factor f, using the uniform distribution. Then, those q models are implemented into the ChemKin solver, with the prescribed initial conditions of the i^{th} data point, and the solver will generate q ChemKin outputs, $\eta_{resp}^{(i)} \in R^{q \times 1}$. Consulting Eqn. (3), we can solve for the coefficients c, b, and A. A simple approach is to first map the feature x into a new vector $\phi(x)$:

$$\phi(x) = [1, x_1, x_2, \ldots, x_n, x_1x_1, x_1x_2, \ldots, x_nx_n]^T \qquad (9)$$

and then solve for the coefficients c, b, and A through normal equations. In the current work, we increase the q value from 200 to 1000, and also generate 20% of q more random samples as test sets. The learning curve is shown below in Figure 3. In detail, Table 2 summarizes the averaged training and test errors with different q values over the entire experimental data set. When q_{train} reaches 1000, both the training and test error falls below 1%, which is good enough for response surface accuracy. Figure 4 also shows the 45-degree plots of one experimental condition case, and both the training and test plots are presented. Indeed, the result confirms that when q_{train} = 1000 for each experimental condition, the model response $\eta_{resp}^{(i)}$ from ChemKin solver can be accurately replaced by its second-order-polynomial response surface.

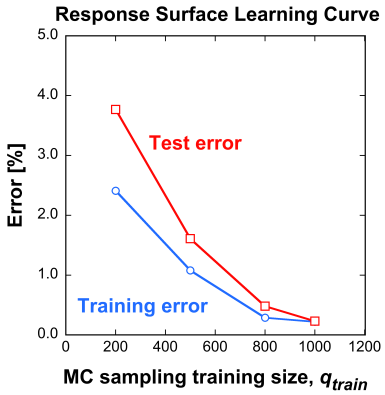

Figure 3. The learning curve of response surface generation.

Table 2. Training and test errors.

Case No.	1	2	3	4
q_{train}	200	500	800	1000
q_{test}	20	100	160	200
Training error (%)	2.41	1.08	0.29	0.22
Test error (%)	3.77	1.61	0.48	0.23

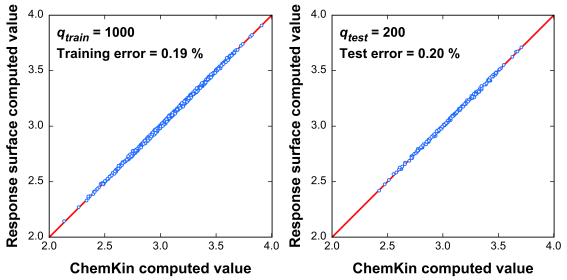

Figure 4. 45-degree plots of one experimental condition for Case 4 (q_{train} = 1000, q_{test} = 200). Left panel: training plot; right panel: test plot.

4.2. Model Optimization

As discussed in Section 3.3, for the first optimization approach, we apply locally weighted least square, considering all the 200 experimental data points as constraints. The update rule for vector x is stochastic gradient descent method.

For the second approach, we implemented the reinforcement learning algorithm. Considering all 200 data points and all 10 effective reactions, the size of the state transition probability matrix P_{sa} is $3^{200}\times3^{200}\times2^{10} \approx O(10^{193})$, which is probably too large and even impossible to store it. In the current work, we are more interested to see whether reinforcement learning works for combustion chemistry model optimization. Therefore, we chose only 5 data points from 2 experiment sets. The resulting size of P_{sa} is $3^5\times3^5\times2^{10} \approx O(10^7)$, which is manageable.

Two selected model validation cases of ignition delay time and laminar flame speed are shown in Figures 5 and 6, respectively. Note that the 5 data points used in reinforcement learning algorithm are just extracted from the datasets in these two figures. Clearly, both figures indicate that the optimized models achieve better prediction accuracy than the unoptimized one. In Figure 5, the two optimized models are indistinguishable in their performances. However, Figure 6 shows that model optimized using the reinforcement learning method actually provides better accuracy than the least square optimized model. The reason is that in the reinforcement learning process, the only success state is that the model prediction for each data point fall within its uncertainty band. However, the experimental uncertainties only serve as weights in the least square approach, not strict constraints.

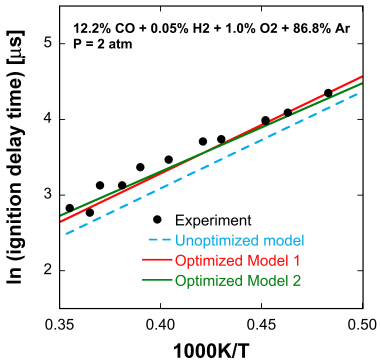

Figure 5. Selected ignition delay time validation of the optimized models

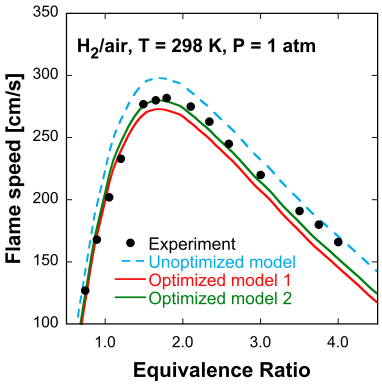

Figure 6. Selected laminar flame speed validation of the optimized models.

The two optimization approaches used herein have their advantages and disadvantages. The locally weighted least square approach is efficient, and is able to handle a large set of data. But the it does not guarantee the optimized model predictions all fall within experimental uncertainties. The reinforcement learning approach, on the other hand, does ensure the model prediction accuracy, but it suffers from its computational efficiency problem and large storage issue.

5. Conclusions and future work

In the current work, we explore two approaches to optimizing a syngas combustion chemistry model. Result shows that the optimized models can improve the prediction accuracy to an extent. One future work is to apply kernel function for response surface generation. Furthermore, it is worthwhile to improve the efficiency and resolve the large storage problem when applying the reinforcement learning method to this combustion chemistry model optimization problem.

References

[1]. Kee, Robert J., Fran M. Rupley, and James A. Miller. Chemkin-II: A Fortran chemical kinetics package for the analysis of gas-phase chemical kinetics. No. SAND-89-8009. Sandia National Labs., Livermore, CA (USA), 1989.

[2]. Tse SD, Zhu DL, Law CK. Morphology and burning rates of expanding spherical flames in H2/O2/inert mixtures up to 60 atmospheres. Proc Combust Inst. 2000; 28:1793–800.

[3]. Burke MP, Chaos M, Dryer FL, Ju Y. Negative pressure dependence of mass burning rates of H2/CO/O2/diluent flames at low flame temperatures. Combust Flame. 2010; 157:618–31.

[4]. Santner J, Dryer FL, Ju Y. The effects of water dilution on hydrogen, syngas, and ethylene flames at elevated pressure. Proc Combust Inst. 2013; 34:719–26.

[5]. Bouvet N, Chauveau C, Gökalp I, Halter F. Experimental studies of the fundamental flame speeds of syngas (H2/CO)/air mixtures. Proc Combust Inst. 2011; 33:913–20.

[6]. Vagelopoulos CM, Egolfopoulos FN. Laminar flame speeds and extinction strain rates of mixtures of carbon monoxide with hydrogen, methane, and air. Symp (Int) Combust. 1994; 25:1317–23.

[7]. Li X, You X, Wu F, Law CK. Uncertainty analysis of the kinetic model prediction for high–pressure H2/CO combustion. Proc Combust Inst. 2015; 35:617–24.

[8]. Hermanns RTE, Konnov AA, Bastiaans RJM, De Goey LPH. Laminar burning velocities of diluted hydrogen–oxygen–nitrogen mixtures. Energy Fuels. 2007; 21:1977–81.

[9]. Dean AM, Steiner DC, Wang EE. A shock tube study of the H2/O2/CO/Ar and H2/N2O/CO/Ar systems: Measurement of the rate constant for H+ N2O= N2+ OH. Combust Flame. 1978; 32:73–83.

[10]. Petersen EL, Davidson DF, Röhrig M, Hanson R. High–pressure shock–tube measurements of ignition times in stoichiometric H2/O2/AR mixtures. In: Sturtevant B, Shepherd JE, Hornung HG, editors. Proceedings of the 20th international symposium on shock waves; 1996; Pasadena, California. p. 941–6.

[11]. Hong Z, Cook RD, Davidson DF, Hanson RK. A shock tube study of OH+ H2O2→ H2O+ HO2 and H2O2+ M→ 2OH+ M using laser absorption of H2O and OH. J Phys Chem A. 2010; 114:5718-27.

[12]. Mueller MA, Kim TJ, Yetter RA, Dryer FL. Flow reactor studies and kinetic modeling of the H2/O2 reaction. Int J Chem Kinet. 1999; 31:113-25.

[13]. Gregory P. Smith, David M. Golden, Michael Frenklach, Nigel W. Moriarty, Boris Eiteneer, Mikhail Goldenberg, C. Thomas Bowman, Ronald K. Hanson, Soonho Song, William C. Gardiner, Jr., Vitali V. Lissianski, and Zhiwei Qin, http://www.me.berkeley.edu/gri_mech/.

[14]. Hai Wang, Xiaoqing You, Ameya V. Joshi, Scott G. Davis, Alexander Laskin, Fokion Egolfopoulos & Chung K. Law, USC Mech Version II. High-Temperature Combustion Reaction Model of H2/CO/C1-C4 Compounds. http://ignis.usc.edu/USC_Mech_II.htm, May 2007.

[15]. Davis, S. G., Joshi, A. V., Wang, H., & Egolfopoulos, F. (2005). An optimized kinetic model of H2/CO combustion. Proceedings of the Combustion Institute, 30(1), 1283-1292.

[16]. Sheen, D. A., You, X., Wang, H., & Løvås, T. (2009). Spectral uncertainty quantification, propagation and optimization of a detailed kinetic model for ethylene combustion. Proceedings of the Combustion Institute, 32(1), 535-542.